Tropospheric Scintillation Spectra and Transversal Wind Speed for Satellite Links at Very Low Elevation Angles

Martin Rytir[1, 2], Carlo Riva[2], Danielle Vanhoenacker-Janvier[3], Terje Tjelta[4]

[1] Norwegian Defence Research Establishment, FFI, Kjeller, Norway, Martin.Rytir@ffi.no

[2] Norwegian University of Science and Technology, NTNU, Trondheim, Norway

[3] Politecnico di Milano, Milan, Italy

[4] Université Catholique de Louvain, UCL, Louvian-La-Neuve, Belgium

[4] Telenor Research and University Graduate Center Kjeller (UNIK), Fornebu, Norway

***Abstract*—Simultaneous measurements of tropospheric scintillation on three different satellite beacons at Ka-band are analyzed. The links have elevation angles of 3.3, 21.2 and 22 degrees. Corner frequency of scintillation is used to calculate the transverse wind speed on each of the links and this is compared with the predictions from a numerical weather model. Results for the two links with higher elevation angle show good agreement with each other as well as with the model data. For the link with elevation angle of 3.3 degrees good match with model data is achieved only when theory applicable for outer scale of turbulence smaller than the Fresnel zone is used. Significant changes in scintillation corner frequency during rain events are also observed for the 3.3 degree link. The results indicate that scintillation at very low elevation angles can be composed of different phenomena, leading among others, to different frequency dependence.**

***Index Terms*—Electromagnetic propagation, scintillation, measurements.**

I. INTRODUCTION

Satellite communication links operating at frequencies higher than a few GHz are significantly affected by tropospheric impairments. Rain is usually the main attenuation source. However, for links with low elevation angles, tropospheric scintillation and multipath can cause large amplitude variations that can be of the same order of magnitude as is typical for rain attenuation.

Several measurements performed at very low elevation angles [1]-[4], have shown scintillation spectra with scintillation corner frequencies f_c much lower than what is typically measured at higher elevation angles [5]-[7]. An explanation based on scintillation theory [8], was proposed in [9]. According to the theory, there are two distinctive cases, depending on the size of the Fresnel zone $\sqrt{\lambda L}$ (where λ is the wavelength and L is the path length trough turbulence), relative to the outer scale of turbulence L_0. For very low elevation angle satellite links L_0 can be smaller than $\sqrt{\lambda L}$, leading to different scintillation spectra. The frequency and path length dependence of the scintillation amplitude is also different for the two cases.

Knowledge of the scintillation spectrum encountered on these links is important for proper implementation of Fade Mitigation Techniques (FMTs). Development of channel simulators for these systems also needs to apply correct theory to produce representative results.

In this paper data from simultaneous measurements at Kjeller, Norway towards three different geostationary satellites are analyzed and their spectra compared with meteorological model predictions. The goal is to identify the cause of the differences in spectra for the different elevation angles. The three links have elevations angles of 3.3, 21.2 and 22 degrees respectively, enabling direct comparison of the spectra at different elevation angles. All links operate at Ka-Band with only minor differences in frequency (20.68, 20.2 and 19.68 GHz). The rest of the paper is organized as follows: Section II summarizes the relevant theory. Section III describes the measurement setup. Section IV shows the data processing for the beacon and meteorological model data. In Section V the results are compared and some examples shown. Section VI draws conclusions.

II. THEORY AND MODELS

A. Scintillation

In [8] three distinct cases for the amplitude variations of a wave propagating in a turbulent medium are found, depending on the size of the first Fresnel zone ($\sqrt{\lambda L}$) relative to the dimensions of the turbulence. The first case is valid for Fresnel zone smaller than the inner scale of turbulence l_0 and will not be discussed here as the value of l_0 in the atmosphere is on the order of a few millimeters.

Case 1) valid for $L_0 > \sqrt{\lambda L}$

For this case, the variance of the log-amplitude fluctuations is given by

$$\sigma^2 = 23.39\, {C_n}^2 \left(\frac{2\pi}{\lambda}\right)^{7/6} L^{11/6} \quad (dB^2) \qquad (1)$$

where ${C_n}^2$ is the refractive index structure parameter. The relationship between the transverse wind speed v_t and the corner frequency of the scintillation f_c for a point receiver is according to [10] given by

$$v_t = \frac{fc}{1.43} \sqrt{2\pi\lambda L} \quad (2)$$

Case 2) valid for $L_0 < \sqrt{\lambda L}$

The variance of log-amplitude fluctuations is given by

$$\sigma^2 = 29.50\, C_n{}^2 \left(\frac{2\pi}{\lambda}\right)^2 L\, L_0{}^{5/3} \quad (dB^2) \quad (3)$$

Transverse wind speed is then calculated using

$$v_t = f_c\, 2\pi\, L_0 \quad (4)$$

For both cases the effect of averaging over antenna aperture has to be accounted for as given by [10] and [11]. The measured corner frequency for a parabolic antenna f_c' is given by

$$f_c' = \frac{e^{-1}\,\Gamma(n/2)}{\xi^2(x)\Gamma((n-1)/2)} f_c \quad (5)$$

where Γ is the gamma function, n=11/3 and $\xi^2(x)$ is the antenna averaging function given by:

$$\xi^2(x) = \frac{14}{3} x^{4/3} - 2(1+x^2)^{\frac{7}{6}} \sin\left(7/3 \operatorname{atan}\left(\frac{1}{x}\right)\right) \quad (6)$$

with

$$x = 0.0584\, \frac{D_e{}^2 2\pi}{\lambda\, L} \quad (7)$$

where D_e is the effective diameter of the antenna.

B. Satellite link considerations

The validity of (1) and (3) at millimeter waves was confirmed by measurements on a 4.1 km terrestrial link in [12]. On a ground-satellite path the signal will encounter most significant turbulence in the lowest part of the atmosphere. The size of the Fresnel zone within the turbulent layer increases from λ/4 at the antenna up to a maximum at the top of the layer. Furthermore a link with a low elevation angle has a longer path length trough the turbulent layer with a correspondingly larger Fresnel zone. For a turbulent height of 2.5 kilometers a link with 20° elevation will have a maximum Fresnel zone size of 10.5 m, while this increases to 26 m for 3° elevation.

The atmosphere typically exhibits a layered structure leading to anisotropic inhomogenities, with much smaller vertical dimension compared with horizontal [13], [14]. L_0 is typically assumed to achieve values between a few meters and about 100 m in the lower atmosphere [15]. During measurements on a 7.5 km terrestrial slant path in Bern, Switzerland [16], median values of 8 meters for the horizontal L_0 and 1.3 m for vertical L_0, were recorded. It was also shown that L_0 can change more than an order of magnitude over just a few minutes. As illustrated in Fig. 1, it is therefore quite likely that for very low elevation angles L_0 can often be smaller than the Fresnel zone for some sections of the path.

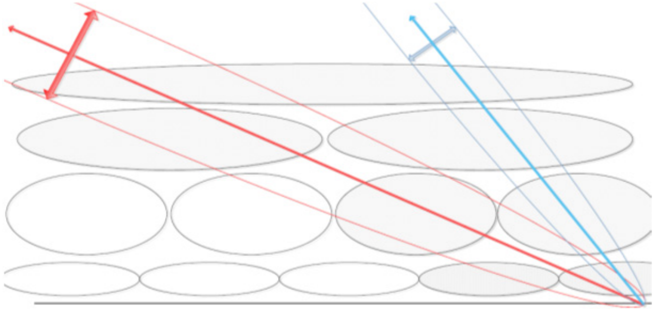

Fig. 1. Slant-path trough anisotropic turbulence for links with different elevation. Fresnel zones for both links are highlighted. Drawing partly based on turbulence model suggested in [13]. All dimensions not to scale.

C. Model implications

Comparing the formulas for the two cases (1), (3) we see that both the frequency and path length dependence are quite different. The frequency exponent changes from 7/6 for case 1) to 2 for case 2) while the path length dependence changes the opposite way from 11/6 to 1. Due to the large and fast variations of L_0 the frequency dependence of low elevation links is therefore likely to vary between these two values, all depending on the position and dimensions of the turbulence. During periods with very small L_0 values this effect might also be encountered on links with higher elevation angles.

This is, at present, not accounted for in the most used prediction models. As an example the ITU-R [17] model for elevation angles over 5° uses 7/6 for the frequency dependence exponent, while the Karasawa model [18] uses empirically derived value of 0.9. Comparative analysis of frequency scaling measured during different experiments [19], reported widely different values and suggested that this might be due to a mixing of different scintillation mechanisms. The existence of a mixture of cases 1) and 2) at low elevation angles is such a mechanism. Frequency scaling measurement done on a 11.2 GHz satellite link with 3.3°, showed a scaling factor varying between 7/6 and 2 [20].

Another mechanism relevant for very low elevation angles is multipath propagation. Multipath can be caused by surface reflection (surface multipath) or by reflections in a layered atmosphere (atmospheric multipath) [14]. The severity of atmospheric multipath is not very dependent on frequency as reflected by the frequency exponent of the multipath part of the ITU-R model [17], which has a value of 0.9.

III. Measurement Setup

A. Beacon Measurement

Three independent simultaneous measurements towards three different geostationary satellites were conducted at Kjeller, Norway with elevation angles of 3.3., 21.2 and 22 degrees respectively. All stations utilized a parabolic antenna and a spectrum analyzer (2 Agilent CXA, 1 R&S FSU) as a beacon receiver. The general setup was the same as described in detail in [21]. Sampling rate of the different measurements was 10 samples/second for the Inmarsat and Ka-Sat measurements and 14 samples/second for the Astra

3B measurement. The main parameters of the measurements and their signal to noise ratio (SNR) are summarized in Table I. In Fig. 2, the distance through the first 2.5 km of atmosphere is illustrated for all links.

B. Meteorological Model

AROME MetCoOp numerical meteorological prediction model data provided by the Norwegian Meteorological Institute (MET) were retrieved for the same period as the beacon measurements. The model uses a grid with 2.5 km resolution and 65 model levels. The time resolution is 1 hour and a new prediction is done for 66 hours 4 times per day. Only a reduced set with data at 11 pressure levels was available for this work.

IV. Data Processing

A. Beacon Data

As a first step all beacon data are controlled using both automatic and manual procedures and invalid data are removed. All data are then resampled with a new sampling frequency of 10 Hz. Averaged spectrum of the signal is calculated for every 30 minutes using overlapping 10 minute blocks for the two links with higher elevation angle, while for the link with lowest elevation it is averaged for every 60 minutes using 20 minute blocks. These period lengths are optimal for identifying corner frequencies at the different elevation angles. From each spectrum the scintillation corner frequency is identified using a semi-automatic procedure. The procedure uses polynomial curve-fitting to approximate the shape of the spectrum and then compares the shape of the polynomial with the expected slope (-8/3 dB/dec) and plateau of scintillation. Periods where corner frequency was difficult to identify were removed from the data.

After the corner frequency is found the transverse wind speed v_t is inferred using (5) and then (4) or (2) respectively as was done in [22]. The height of the turbulence is assumed to be from ground up to 500 m below the 0° C isotherm for the two months of measurement, giving about 2.5 km.

TABLE I. Main Parameters of the Three Measurements

Satellite	*Frequency [GHz]*	*Elevation [°]*	*Azimuth [°]*	*Antenna Diameter [m]*	*SNR [dB]*
Inmarsat-5 F2	20.68	3.3	249	1.2	47
Astra 3B	20.199	21.2	165.7	2.4	59
Ka-Sat	19.68	22	182.4	1.2	37

Fig. 2. Path trough first 2.5 km of atmosphere towards Inmarsat-5 F2 (39 km) in red, Astra 3B (6.5 km) in yellow and Ka-Sat (6.3 km) in blue.

B. Meteorological Model Data

First 3 hours of each prediction were discarded as recommended by MET. The following 6 hours were used until data from the next prediction were available. The eastward, northward and vertical wind speed components were then interpolated along the path for each hour. The path was sampled every 300 meters and at each of the points the value was interpolated by first using Barycentric interpolation from 3 nearest points above and below the current height and then using linear interpolation between these two values. Absolute value of the transversal wind speed (speed in the plane perpendicular on the propagation direction), was then calculated for each of the points. Finally the transversal wind speed along the whole path is taken as a mean of these absolute values.

V. Results

The total number of periods with identified corner frequencies for July and August 2016 was: 2814 for the Astra 3B beacon, 2040 for the Ka-Sat beacon (both for 30 min intervals) and 1330 for the Inmarsat 5-F2 (60 min intervals).

Since the Astra 3B and Ka-Sat links have nearly identical elevation, frequency and azimuth the transversal wind speed on these links should be about the same. Therefore it is possible to use this data to test the accuracy of both the corner frequency measurement and of the AROME model data. Example of a direct comparison over a few days is shown in Fig. 3. The beacon-derived data, calculated using (2), match extremely well. The model data have a bit lower values and do not follow the fast changes during the period of strong winds on 16th and 17th of July. On the 15th of July it seems that the model predicted a period of slightly stronger winds a few hours earlier. However, overall both the model data and the AROME data fit quite well.

A scatterplot of the Ka-Sat and AROME data is shown in Fig 4. As could be expected when comparing prediction data with measurements, there is some spread in the values, there is also a clear offset with measured wind speed being some 1.7 m/s higher than predicted, nevertheless the overall correlation is still quite high. Complementary cumulative distribution functions (CCDFs) of the 4 datasets are compared in Fig 5 highlight the higher measured values relative to the model.

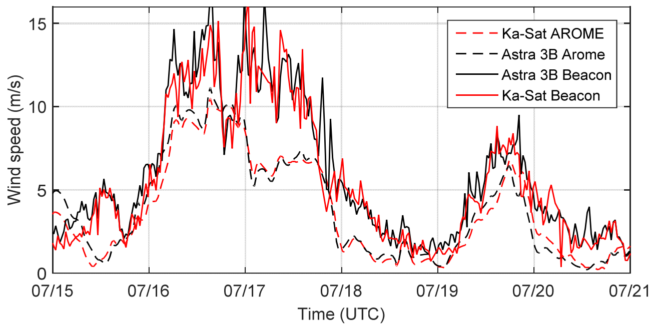

Fig. 3. Transverse wind speed for the Ka-Sat and Astra 3B links calculated from spectra compared with AROME MetCoOp model data.

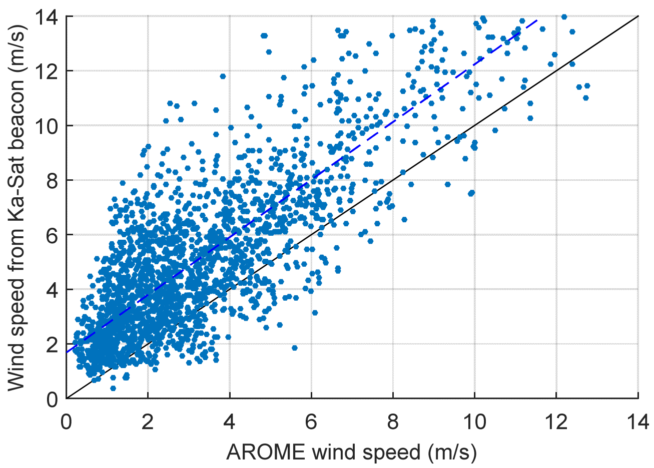

Fig. 4. Transverse wind speed calculated from beacon spectra compared with wind speed from the AROME MetCoOp model for the Ka-Sat link (22° elevation). Dashed blue line is a linear fit of the data.

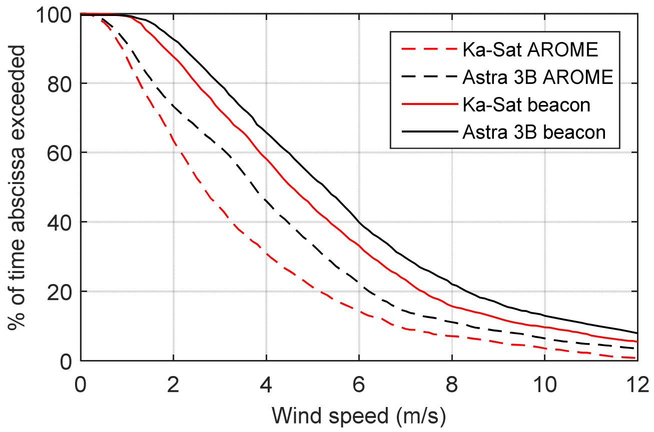

Fig. 5. CCDF comparison of the wind speeds inferred from spectra and given by the AROME MetCoOp model)

As shown in Figs. 6 and 7, similar calculation using (2) for the 3.3° elevation link, gives much lower values than predicted by the model, which is opposite of what Figs. 4 and 5 show. Assuming that Case 2) ($L_0 < \sqrt{\lambda L}$) is valid and using (4) with constant L_0 = 13 m, the values are much closer. Unsurprisingly, constant L_0 causes rather large spread in the data in Fig 6. By taking the AROME windspeed and measured f_c, and calculating the L_0, we get approximately log-normal distribution (μ=2.59, σ=0.68) with a median of 14 m. It should be noted that we still assume constant turbulent height of 2.5 km.

We also observed that during some periods of increased rain attenuation the windspeed calculated for Case 2) using constant L_0 was much higher than the AROME value, while the value calculated for Case 1) was much closer. An example of such an event is shown in Fig. 8, clearly showing how the amplitude of scintillation decreases and the corner frequency increases during severe attenuation. A possible explanation is that the L_0 gets much smaller (3-4 meters) during these periods.

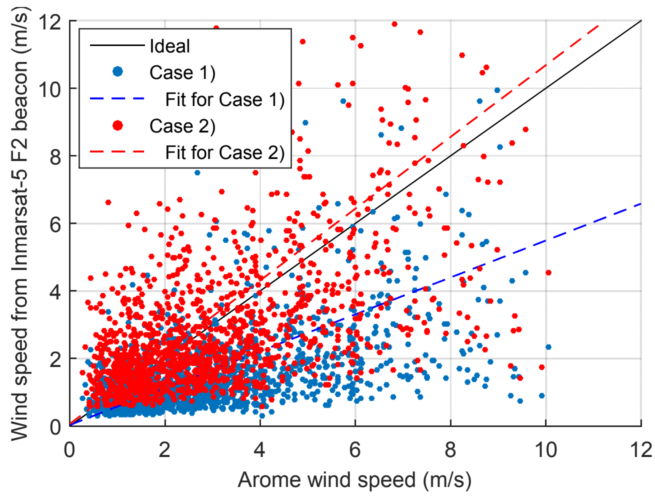

Fig. 6. Transverse wind speed calculated from beacon spectra compared with wind speed from the AROME MetCoOp model for the Inmarsat-5 F2 link (3.3° elevation) using two different formulas.

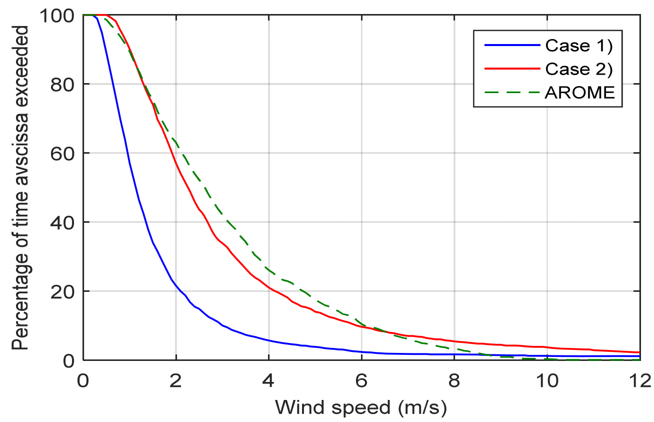

Fig. 7. CCDF comparison of the wind speed inferred from spectra and given by the AROME MetCoOp model for the Inmarsat-5F2 link.

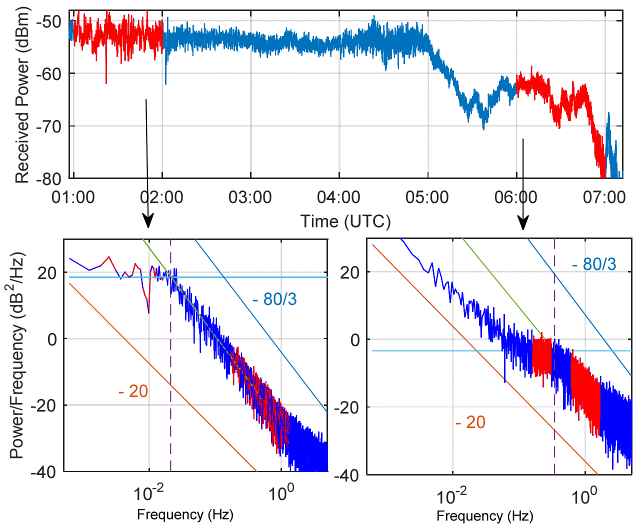

Fig. 8. Example of Inmarsat-5 F2 beacon spectra on 08/08/2016. The theoretical slopes of scintillation (-80/3 dB/dec) and attenuation (-20) are also shown. The green and light blue lines denote the asymptotes whos intersection defines the corner frequency (marked as dashed line). The red parts of the spectrum show the areas used for calculation of the asymptotes.

VI. CONCLUSIONS

Two months of simultaneous measurements of three different satellite beacons at one site were analyzed and compared with numerical weather model data. The transversal wind speed calculated on the assumption that the outer scale of the turbulence L_0 is larger than the Fresnel zone ($L_0 > \sqrt{\lambda L}$), from the two beacons with 21.2° and 22° elevation angle, shows very good agreement with each other and good agreement with the model data. Here the meteorological model data always predicts higher wind speed than measured; this is likely caused by averaging in the model. The scintillation corner frequencies found for the link with 3.3° elevation angle are typically an order of magnitude lower than those for the two other links. Transversal wind speed calculated for this link using the same formulas shows poor match with the meteorological model with consistently lower values. If we instead use formulas valid for Fresnel zone larger than the turbulence outer scale ($L_0 < \sqrt{\lambda L}$) we get a good match. Data collected during periods with rain attenuation indicate that the turbulence outer scale probably changes significantly during these events.

The obtained results seem to show that for very low elevation angle links scintillation should most of the time follow the theory for Fresnel zone larger than the turbulence outer scale. This could have significant impact on the frequency and path length dependence of the amplitude of the scintillations. Depending on the position and strength of the turbulent layer, similar situation can also happen for parts of satellite links at higher elevation angles. However, it should be noted that the spectra at the low elevation angles are also affected by atmospheric multipath which cannot be easily separated from scintillation.

ACKNOWLEDGMENT

The authors would like to thank Terje Mjelde and Jostein Sander at FFI for help in preforming the measurements, Lars Bråten from FFI for comments and recommendations. The Norwegian Meteorological Institute provided the AROME MetCoOp model data. Cyriac de Villenfagne from UCL created the software for retrieving the corner frequency while Laurent Quibus from the same institution helped with the meteorological data retrieval.

REFERENCES

[1] J. R. Larsen, "Investigation of the relative contributions of propagation phenomena on an 11 GHz satellite link at 5 deg elevation," *5th International Conference on Antennas and Propagation (ICAP)*, York, pp. 145-148, March/April 1987.

[2] E. C. Johnston, D. L. Bryant, D. Maiti and J. E. Allnutt, "Results of Low elevation angle 11GHz satellite beacon measurements at Goonhilly," 7th *International Conference on Antennas and Propagation (ICAP*), vol. 1, pp. 366-369, 1991.

[3] P. T. Thompson and B. G. Evans, "Results of Simultaneous Very Low Elevation Ku-Band Propagation Measurements at Two Sites in Southern England," *30th AIAA International Communications Satellite System Conference (ICSSC)*, Ottawa, September 2012,

[4] M. Rytir, "Clear-Air Scintillation and Multipath for Low-Elevation High-Latitude Satellite Communication Links," *In Proc. 9th European Conference on Antennas and Propagation (EuCap)*, Lisbon, pp. 1-5, April 2015.

[5] E. Vilar and J. Haddon, "Measurement and Modeling of Scintillation Intensity to Estimate Turbulence Parameters in an Earth-Space Path," *IEEE Trans. Ant. Prop.*, vol. 32, no.4, pp. 340-346, April 1984.

[6] Y. Karasawa and T. Matsudo, "Characteristics of fading on low-elevation angle Earth-space paths with concurrent rain attenuation and scintillation," *IEEE Trans. Ant. Prop.,* vol. 39, iss. 5, pp. 657-661, 1991.

[7] E. Matricciani, M. Mauri and C. Riva, "Relationship between scintillation and rain attenuation at 19.77 GHz," *Radio Science*, vol. 31, no. 2, pp. 273-279, March-April 1996.

[8] V. I. Tatarski, "Wave Propagation in a Turbulent Medium," McGraw-Hill, New York, 1961.

[9] E. Vilar and J. R. Larsen, "Elevation Dependence of Amplitude Scintillations on Low Elevation Earth Space Paths," *6th International Conference on Antennas and Propagation (ICAP)*, vol. 2, pp. 150-154, 1989.

[10] J. Haddon and E. Vilar, "Scattering Induced Microwave Scintillations from Clear Air and Rain on Earth Space Paths and the Influence of Antenna Aperture," *IEEE Trans. Ant. Prop.,* vol. 34, iss. 5, pp. 646-657, 1986.

[11] M. M. J. L. van de Kamp, J. K. Tervonen, E. T. Salonene and K. Kalliola, "Study of low elevation angle scintillation modelling," ESA Report, September 1997.

[12] R. S. Cole, K. L. Ho and N. D. Mavrokoukoulakis, "The Effect of the Outer Scale of Turbulence and Wavelength on Scintillation Fading at Millimeter Wavelengths," *IEEE Trans. Ant. Prop.,* vol. 26, iss. 5, pp. 712-715, 1978.

[13] A. D. Wheelon, Electromagnetic Scintillation. Part I and II. Cambridge, U.K.. Cambridge Univ. Press., 2003.

[14] Y. A. Kravtsov, "Propagation of electromagnetic waves trough a turbulent atmosphere," *Rep. Prog. Phys.,* vol. 55, n. 1, pp. 39-112, 1992.

[15] R. K. Crane, "A review of radar observations of turbulence in the lower stratosphere," *Radio Sci.*, vol. 15, no. 2, pp. 177–193, 1980.

[16] A. Lűdi and A. Magun, "Near-horizontal line-of-sight millimeter-wave propagation measurements for the determination of outer length scales and anisotropy of turbulent refractive index fluctuations in the lower atmosphere," *Radio Sc.*, vol. 37, no. 2, pp. 12-1-12-19, April 2002.

[17] ITU-R Recommendation P.618-12, "Propagation data and prediction methods required for the design of Earth-space telecommunication systems," International Telecommunication Union, Geneva, Switzerland, 2015.

[18] Y. Karasawa, M.Yamada and J.E. Allnutt, "A new prediction method for tropospheric scintillation on earth-space paths," *IEEE Trans. Ant. Prop.,* vol.36, Nov. 1988.

[19] M. M. J. L. van de Kamp, C. Riva, J. K. Tervonen and E. T. Salonen, "Frequency Dependence of Amplitutde Scintillation," *IEEE Trans. Ant. Prop.,* vol. 47, no. 1, pp. 77-85, January 1999.

[20] S. M. R. Jones, I. A. Glover, P. A. Watson and R. G. Howell, "Evidence for the Presence of Turbulent Attenuation on Low-Elevation Angle Earth-Space Paths – Part 2: Frequency Scaling of Scintillation Intensity on a 10° Path," *IEEE Trans. Ant. Prop.,* vol. 45, no. 1, pp. 85-92, January 1997.

[21] L. E. Bråten, J. Sander and T. Mjelde, "Satellite-Earth K-band Beacon Measurements at Kjeller, Norway; Measurement setup and initial results," *In Proc. 7th European Conf. Ant. and Prop. (EuCap)*, Gothenburg, 8-12 April 2013.

[22] C. Riva, L. Luini, J. Nessel and M. Rytir, "Wind Intensity Inferred from Alphasat Ka- and Q-band beacon measurements," *In Proc. 10th European Conference on Antennas and Propagation (EuCap)*, Davos, pp. 1-4, April 2016.